

Study on Mixed Convection Heat transfer in Vertical ducts with Radiation effects

G.Rajamohan, N.Ramesh and P.Kumar

Abstract—Experiments have been performed to investigate the radiation effects on mixed convection heat transfer for thermally developing airflow in vertical ducts with two differentially heated isothermal walls and two adiabatic walls. The investigation covers the Reynolds number $Re = 800$ to $Re = 2900$, heat flux varied from 256 W/m^2 to 863 W/m^2 , hot wall temperature ranges from 27°C to 100°C , aspect ratios 1 & 0.5 and the emissivity of internal walls are 0.05 and 0.85. In the present study, combined flow visualization was conducted to observe the flow patterns. The effect of surface temperature along the walls was studied to investigate the local Nusselt number variation within the duct. The result shows that flow condition and radiation significantly affect the total Nusselt number and tends to reduce the buoyancy condition.

Keywords—Mixed convection, Vertical duct, Thermally developing and Radiation effects

I. INTRODUCTION

MIXED convection heat transfer for thermally developing airflow in vertical ducts is encountered in a wide range of thermal engineering applications such as cooling of electronic equipment, compact heat exchangers, solar collectors and thermal-energy conversion devices. The performance of thermal energy conversion devices depends on the nature of heat dissipation and the operation modes of the system. An understanding of the various fluid flow and heat exchange processes enables efficient design of these devices. Therefore, research on flow and heat transfer through ducts requires significant attention. The amount of heat energy transported by the working fluid in a duct is dependent on the geometry of the duct, nature of the flow, and the thermal boundary conditions of the duct. Air is a common working fluid, and is widely preferred as the medium for cooling of electronic equipment, due to the advantages in handling air and its cost effectiveness. The application potential of vertical ducts underscores the importance of the study of mixed convection with surface radiation effects. Comprehensive review of experimental and theoretical studies has been presented on mixed convection heat transfer in internal flows [1-2]. Numerical investigation of mixed convection heat transfer in airflow through a horizontal rectangular duct with radiation effects [3] and experimental investigation of mixed convection heat transfer for thermally developing flow in horizontal ducts with radiation effects [4] show the variation

of Nusselt number, flow patterns and significance of radiation effects. It was also found that the surface radiation heat transfer along with mixed convection helps to improve the total heat transfer rate. Combined forced and free convection in a vertical rectangular duct [5] with prescribed wall heat flux has been numerically investigated. Numerical investigation has also been done on fully developed mixed convection flow with dual mixed convection flow in a vertical channel [6]. Experimental work has been carried out to study the behavior of mixed convection flow in a channel heated from one side wall [7-8]. Mixed convection laminar flow between parallel plates heated uniformly from below was investigated [9-10] and correlations were suggested for the fully developed Nusselt numbers and for the locations of the onset of secondary flow. Same type of test section presented both theoretical and experimental work on natural convection and radiation in square enclosure [11]. Considerable experimental research has been done by many researchers [12-13] on bottom heated horizontal ducts, horizontal circular cylinders, aspect ratio effects in horizontal duct, hydrodynamically and thermally developed flow in horizontal circular cylinder and rectangular channel with discrete heat sources. A careful review of the above literature shows that a lot of experimental work is still required to be done to examine the effect of mixed convection heat transfer in vertical ducts with radiation effects heated from side wall.

II. EXPERIMENTAL APPARATUS AND PROCEDURE

The experimental apparatus is schematically illustrated in Fig. 1. It consists of a centrifugal blower with speed-regulator, test section, measuring probes, data acquisition system, test cell, and a power supply unit. The blower is used to provide forced air flow to the test section. The flow rate is measured by using an anemometer (Testo 425) with an accuracy of $\pm 1.5\%$. Two test sections were designed and fabricated to be used in the test rig. These test sections can be removed or attached as and when required. Two test-sections were separately investigated in the present set of experiments. Table I shows the dimensions of the test section and flow conditions.

TABLE I
DIMENSIONS OF THE TEST SECTION

AR	W (m)	H (m)	L (m)	D_h (m)	U (m/s)	Re
1	0.054	0.054	0.270	0.054	0.24	858
1	0.054	0.054	0.270	0.054	0.50	1788
1	0.054	0.054	0.270	0.054	0.80	2861
0.5	0.027	0.054	0.270	0.036	0.36	858
0.5	0.027	0.054	0.270	0.036	0.75	1788
0.5	0.027	0.054	0.270	0.036	1.20	2861

G.Rajamohan is with the school of Engineering and Science, Curtin University, Sarawak, Malaysia. (phone: 60-85-44 3832; fax: 60-85-44 3838; e-mail: rajamohan.g@curtin.edu.my).

N.Ramesh is with the department of Mechanical Engineering, Curtin University, Perth, Australia. (phone: 60-85-44 3832; fax: 60-85-44 3838; e-mail: R.Narayanaswamy@exchange.curtin.edu.au).

P.Kumar is with the school of Engineering and Science, Curtin University, Sarawak, Malaysia. (e-mail: p.kumar@curtin.edu.my).

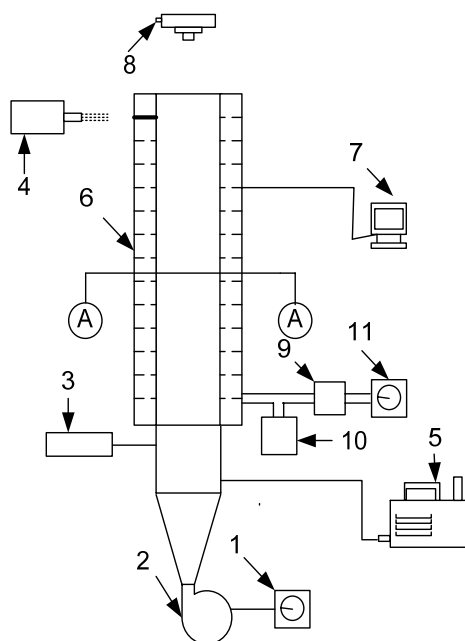


Fig. 1 Schematic diagram of the experimental rig shown with various components (1. DC power supply, 2. blower, 3. anemometer, 4. illuminator, 5. smoke generator, 6. test section, 7. data acquisition system, 8. camera, 9. voltmeter, 10. ammeter, 11. AC power supply.)

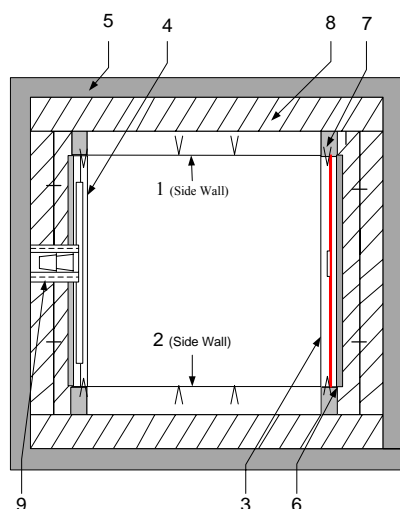


Fig. 2 Sectional (A-A) diagram of 54 mm x 54 mm experimental test cell (1 & 2. adiabatic walls, 3 & 4. isothermal hot and cold walls, 5. insulation, 6. electric heater, 7. thermocouples, 8. wood, 9. water circulation port)

Figure 2 shows the schematic of square cross-section of the test section. The test section is made of two differentially heated isothermal walls and two adiabatic walls. The isothermal hot wall incorporates an electrical heater made of silicon rubber and isothermal cold walls incorporates a milled-channel to circulate constant temperature water provided by a thermostat with fuzzy control system (Wisecircu, flow rate – 6 litre/min, $\pm 0.05^\circ\text{C}$) to act as a constant temperature sink. The inside surface of the cold wall and the hot wall are highly polished in order to achieve a mirror finish, to have a low

emissivity of 0.05, or coated with blackboard paint to have an emissivity of 0.85[4].

K-type thermocouples were fixed in the hot, cold and side walls at various locations along the length (inlet to outlet) direction, for measuring the respective wall temperatures. The thermocouples were made of 0.3 mm diameter wire, and were embedded in holes drilled much closer to the polished surface of the wall. The thermocouples were fixed using thermally conducting cement. All the thermocouples were calibrated over the range considered in the present study.

The two side walls made of Perspex are milled, based on the design requirement for the two different aspect ratios. Conduction heat transfer between the walls was minimized. Glass-wool insulation material was filled in all corners of the test section to avoid air circulation in the slots. Thermocouples were embedded on the inside and outside surface of the side walls to measure temperature. This was done in order to obtain the temperature distribution along the inside of the two side walls, and to estimate the conduction heat loss via the two side walls. The side walls were painted black (on the inside surface) in order to obtain a surface emissivity of about 0.85 or provided with very thin aluminum foil (on the inside surface) so as to obtain a surface of emissivity of about 0.05.

A typical experimental run consisted of maintaining the different flow conditions with desired temperatures for the hot and cold walls, starting the blower, attaining steady state conditions and then recording a set of data. The cold wall temperature is always maintained to be equal to the inlet air temperature throughout an experiment, and for all experiments considered in this study. Flow visualization was also conducted to observe qualitative pattern of the flow. A smoke generator was used to supply the smoke to the test section through a 1.5 mm slot created at the bottom of the test section entrance at a suitable location closer to the exit of the duct. When illuminated through the top wall by an illuminator (LB Cold beam 5W Illuminator) and viewed from the end of the front test section, a sharp contrast could be achieved between walls and the smoke. The smoke particle size (mass median diameter) range is 0.2 - 0.3 micron and this range was able to trace the flow in the duct [4].

III. EXPERIMENTAL UNCERTAINTY

Uncertainty analysis was conducted to ascertain the accuracy and reliability of the experimental results. Uncertainties were estimated according to the procedure [15]. The overall uncertainty in the estimated Nusselt number from the heated wall of the test section was found to be less than $\pm 3.5\%$, for the range of Reynolds numbers considered in this study.

IV. RESULTS AND DISCUSSION

Numbers of test runs have been conducted to cover the Reynolds number $Re = 800$ to $Re = 2900$, the heat flux varied from 256 W/m^2 to 863 W/m^2 , hot wall temperature ranges from 27°C to 100°C , aspect ratios 1 & 0.5 and the emissivity of internal walls are 0.05 and 0.85. The experimental data was analyzed to obtain various heat transfer quantities due to mixed convection and surface radiation heat transfer from the hot vertical wall of the duct. To obtain the radiation heat transfer from the hot wall, a

numerical modeling method using the computational fluid dynamics solver FLUENT was chosen to create a geometrical simulation of the enclosure. The experimentally observed walls temperature was used as input quantities in the numerical modeling, thereby providing most accurate results in this analysis.

The convection heat transfer from the hot wall surface is obtained as

$$Q_{conv} = Q_t - Q_{cond} - Q_{rad} \quad (1)$$

Where, Q_{cond} is the conduction heat transfer from the hot vertical wall. Q_{rad} is the radiation heat transfer from the heated wall, which is obtained from the numerical analysis. For all the cases considered in this study, the conduction heat transfer rate across the hot wall was found to be very small and negligible. The convection heat flux from the vertical wall is calculated from:

$$q_{conv} = Q_{conv} / A_s \quad (2)$$

where $A_s = H \times L$

The average convective Nusslet number at the heated wall is calculated based on the hot wall surface temperature and the mean temperature of air as follows:

$$Nu_{conv} = q_{conv} D_h / (T_h - T_m) k_m \quad (3)$$

where,

$$T_m = (T_{in} + T_{out}) / 2 \quad (4)$$

The average radiative Nusselt number at the hot vertical wall is given as

$$Nu_{rad} = q_{rad} D_h / (T_h - T_m) k_m \quad (5)$$

The total Nusselt number at the heated vertical wall is given as

$$Nu_{total} = Nu_{conv} + Nu_{rad} \quad (6)$$

A. Surface temperature distribution along the walls

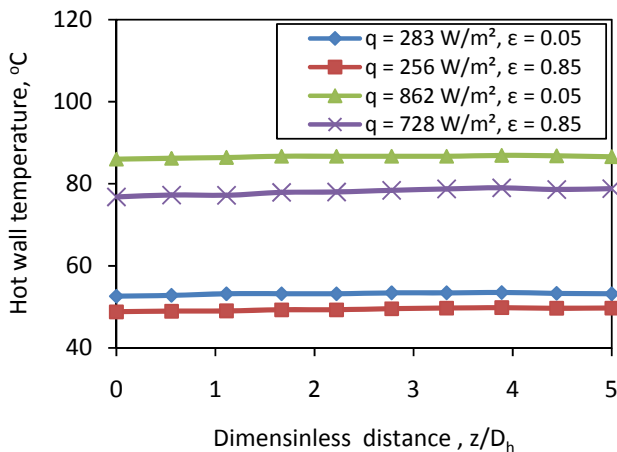


Fig. 3 Variation of the surface temperature on the heated wall for Re = 1788, AR = 1

Fig. 3-6 show the surface temperature distribution on the duct walls for selected runs. Normally, the variation of the surface temperature along the duct depends on heat flux, emissivity of walls, Reynolds number and the flow condition.

Fig. 3 shows the variation of surface temperature on the heated wall inside temperature as a function of the horizontal distance from the inlet of the test section to the exit. The graphs show the variation of surface temperature on the heated wall temperatures for a low and high heat flux with different emissivity for $Re = 1788$. All the graphs show that the variation of the surface temperature along the heated wall is uniform. Fig. 4 shows that the cold wall temperature has almost same temperature as the inlet air temperature and it is maintaining the same condition for all cases.

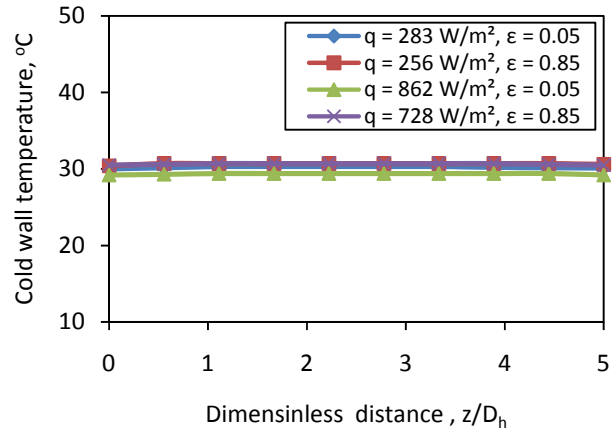


Fig. 4 Variation of the surface temperature on the cold wall for Re = 1788, AR = 1

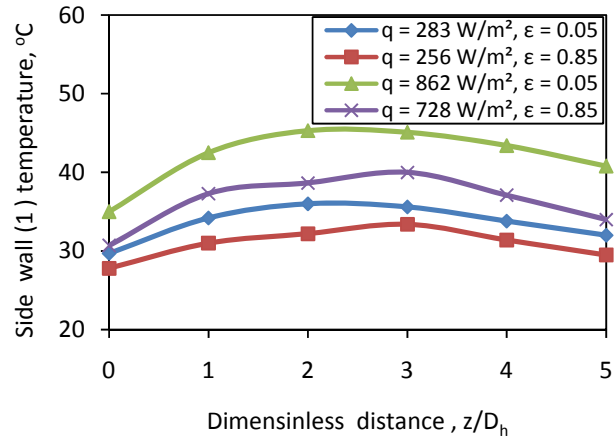


Fig. 5 Variation of the surface temperature on the top wall for Re = 1788, AR = 1

The Fig. 5 and 6 show the variation of the side walls inside temperature as a function of the vertical distance from the inlet of the test section to the exit for Reynolds number of 1788. It can be seen from the fig. that both the side walls maintain the same temperature for the whole length of the duct. The average of side wall temperature is almost independent of the surface emissivity of the duct walls. For a particular value of the input wall heat flux, the temperature drop per unit length of the test section from the inlet to the outlet of the duct is found to be the same for all cases. The differences in the side walls temperature are due to the result of the interaction of the mixed convection effects and the surface radiation effects. For

mixed convection cases having a strong natural convection heat transfer component, the average of side walls temperature is always same.

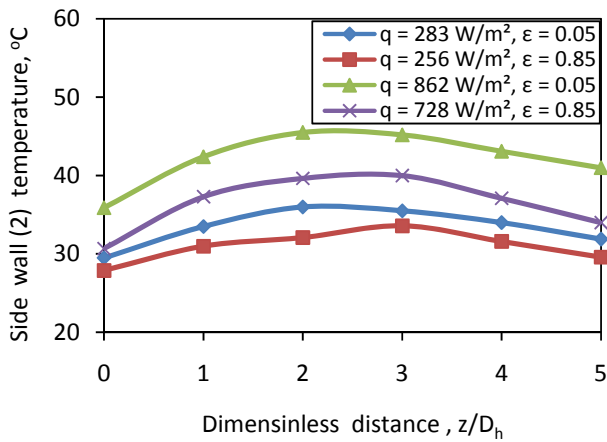


Fig. 6 Variation of bottom wall temperature distribution with the dimensionless distance for $Re = 1788$, $AR = 1$

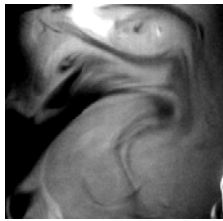


Fig. 7 Mixed convection flow structure within square duct

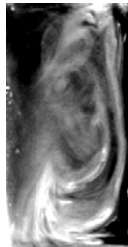


Fig. 8 Mixed convection flow structure within Rectangular duct

The flow visualization photographs provide a picture of the flow field as seen at a cross-section of the test section. Fig. 7. Shows the mixed convection flow structure for square duct. This is for a case with $Re = 858$, $AR=1$ and $\epsilon = 0.05$, the hot wall (right) was maintained at 95.6°C and cold wall (left) at 31°C . Figure 8 shows the mixed convection flow structure for rectangular duct. This is for a case with $Re = 858$, $AR=0.5$ and $\epsilon = 0.05$, the hot wall (right) was maintained at 97.4°C and cold wall (left) at 31.3°C . As the flow is induced by buoyancy, it starts to move upward to the z direction of the vertical duct.

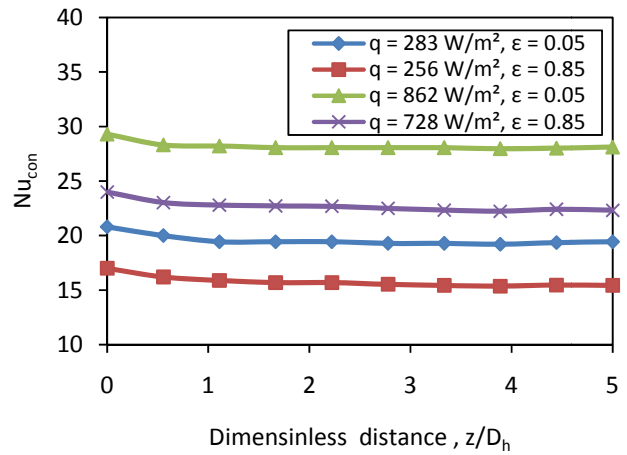


Fig. 9 Effect of Emissivity and heat flux on the average convective Nusselt number at heated wall for $Re = 1788$, $AR = 1$

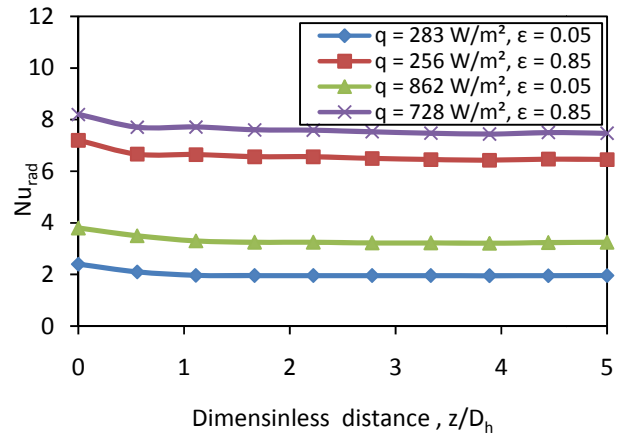


Fig. 10 Effect of Emissivity and heat flux on the average radiative Nusselt number at heated wall for $Re = 1788$, $AR = 1$

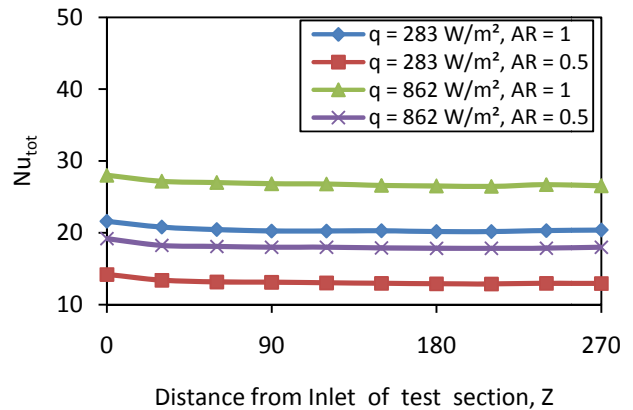


Fig. 11 Effect of Aspect ratio on the average total Nusselt number at heated wall for $Re = 858$, $\epsilon = 0.05$

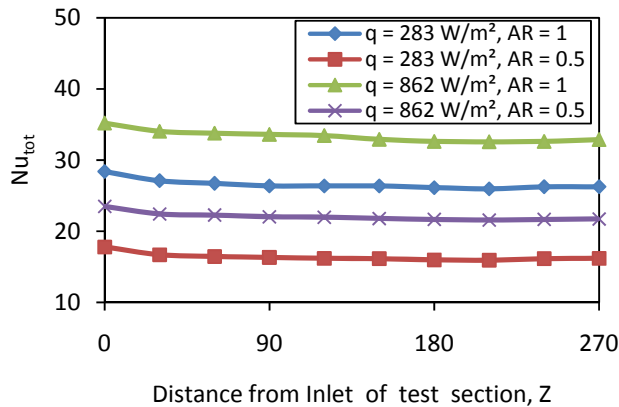


Fig. 12 Effect of Aspect ratio on the average total Nusselt number at heated wall for $Re = 2861$, $\varepsilon = 0.05$

The variation of average convective Nusselt number at the heated wall for a duct of square cross section ($AR=1$) as a function of the Reynolds number with different emissivity of wall is shown in Fig. 9. It is found that for a given wall heat flux, the convective Nusselt number is higher for highly polished surface than that of black surface. Fig. 10 shows the variation of average radiative Nusselt number with Reynolds number for square duct. It is clearly seen that as the average radiative Nusselt number is a very strong function of surface emissivity. Since radiation is a surface phenomenon, dependent on the wall emissivity and the wall temperatures, a reduction in the duct wall temperature causes a reduction in the radiative heat transfer rate. The case of the duct having highly emissive walls, and higher wall fluxes (and temperature) provides a higher value of the average radiative Nusselt number. Considering that the mixed convection and surface radiation effects occur in a coupled mode, the total heat transfer rate from the heated wall can be represented as the sum of the Nusselt numbers due to convection and radiation. This is shown in Fig. 11 and 12, wherein the variation of the average total Nusselt number is plotted as a function of aspect ratio with $Re=858$ and 2861 respectively. It can be seen that for a given wall heat flux, the average total Nusselt number is higher for a higher aspect ratio.

V. CONCLUSIONS

The Nusselt number distributions have been presented at different Reynolds number, different heat fluxes, wall emissivity and aspect ratios. The surface temperature was found to be higher for low Reynolds number due to the free convection effect. Flow visualization results showed that the heated flow moves upward in the Z direction from inlet of test section. Highly polished walls in a vertical duct can be used as a passive heat transfer enhancement method, even in the presence of mixed convection.

ACKNOWLEDGMENT

The first author gratefully acknowledges the financial support for this study from the Curtin Sarawak Research Fund and higher degree research scholarship supported by Curtin University.

REFERENCES

- [1] J.D.Jackson, M.A.Cotton, and B.P.Axcell, "Studies of mixed convection in vertical tubes," *International Journal of Heat and Fluid Flow*, vol. 10, pp.1-15, July 1989.
- [2] W.M.Yan, and H.Y.Li, "Radiation Effects on Mixed convection heat transfer in a vertical square ducts," *International Journal of Heat and Mass Transfer*, vol. 44, pp.1401-1410, Apr. 2001.
- [3] T.T.Chandratilleke, N.Ramesh, and P.Wangdham-koom, "Convective heat transfer in airflow through a duct with thermal radiation," *IOP Conference Series 10 Materials Science and Engineering*, 012026, Jan. 2010.
- [4] G.Rajamohan, N.Ramesh, G.Alexander, and P.Kumar, "Experimental study on mixed convection heat transfer for thermally developing flow in horizontal ducts with radiation effects," *ASME/JSME 8th Thermal Engineering Joint Conference*, 44174, Mar. 2011.
- [5] A.Barletta, E.Rossi di Schio, and E.Zanchini, "Combined forced and free flow in a vertical rectangular duct with prescribed wall heat flux," *International Journal of Heat and Fluid Flow*, vol. 24, pp. 874-887, July 2003.
- [6] A. Barletta, E.Magyari, and B.Keller, "Combined forced and free flow in a vertical rectangular duct with prescribed wall heat flux," *International Journal of Heat and Mass transfer*, vol. 24, pp. 874-887, Aug. 2005.
- [7] C.Gau, Y.C.Jeng, and C.G.Liu, "An experimental study on mixed convection in a horizontal rectangular channel heated from a side," *Transactions of the ASME Journal of Heat Transfer*, vol. 122, pp. 701-707, Nov.2000.
- [8] C.S.Yang, C.G.Liu, and C.Gau, "Study of channel divergence on the flow and heat transfer in horizontal ducts heated from a side," *International Journal of Thermal Sciences*, vol. 48, pp.105-113, Feb.2009.
- [9] J.R.Maughan, and F.P.Incropera, "Experiments on mixed convection heat transfer for airflow in a horizontal and inclined channel," *International Journal of Heat and Mass Transfer*, vol.30, pp.1307-1318, Nov.1987.
- [10] J.R.Maughan, and F.P.Incropera, "Regions of heat transfer enhancement for laminar mixed convection in a parallel plate channel," *International Journal of Heat and Mass Transfer*, vol. 33(3), pp.555-570, Nov.1990.
- [11] N.Ramesh, and S.P.Venkateshan, "Experimental study of natural convection in a square enclosure using differential interferometer," *International Journal of Heat and Mass Transfer*, vol. 44(6), pp.1107-1117, May 2001.
- [12] M.Y.Chang, and T.F. Lin, "Experimental study of aspect ratio effects on longitudinal vortex flow in mixed convection of air in a horizontal rectangular duct," *International Journal of Heat and Mass Transfer*, vol. 41, pp.719-733, May 1997.
- [13] A.Dogan, M.Sivrioglu, and S.Baskaya, "Experimental investigation of mixed convection heat transfer in a rectangular channel with discrete heat sources at the top and at the bottom," *International Communications in Heat and Mass Transfer*, vol. 32, pp.1244-1252, July 2005.
- [14] H.W.Coleman, and W.G.Steele Jr, "Experimentation and Uncertainty Analysis for Engineers," 2nd ed., John Wiley & Sons, New York 275, Mar.1989.